Mechanical characteristics and particle breakage of coral sand under one-dimensional repeated loading

Chunyan Wang[1,2], Xuanming Ding[1,2], Zhenyu Yin[3], Yu Peng[1,2], Zhixiong Chen[1,2*]

1. College of Civil Engineering, Chongqing University, Chongqing, 400045, China

2. Key Laboratory of New Technology for Construction of Cities in Mountain Area, Chongqing University, Chongqing 400045, China

3. Department of Civil and Environmental Engineering, The Hong Kong Polytechnic University, Hung Hom, Kowloon, Hong Kong, China

Abstract: Coral sand, which is an important filler resource in coastal areas, is continuously subjected to repeated waves or traffic loading. In this study, a series of oedometer tests are conducted on coral sand and silica sand under repeated loading, and the results are compared. The influence of the initial density and number and amplitude of repeated loading on the volumetric deformation, soil stiffness, and particle breakage are investigated. The results reveal that the volumetric deformation and particle breakage of coral sand mainly occur in the first loading stage and increase by increasing loading amplitude and reducing initial density. Compared to silica sand, the soil stiffness is lower and volumetric deformation is greater in coral sand during the initial loading stage. However, the opposite trend is observed for the subsequent loading. Finally, three power functions are proposed to predict the volumetric deformation and particle breakage of coral sand under repeated loading.

Keywords: Coral sand, Repeated loading, Particle breakage, Soil stiffness, Silica sand

1. Introduction

In recent years, with increasing tourism and resource exploitation, land reclamation and construction projects on islands have been developing rapidly [1-3]. In many reef island infrastructures, such as airport runways and road pavement, coral sand is used as a foundation filling material due to the shortage of terrestrial filler, which will be subjected to tens of thousands of low frequency repeated traffic and wave loading [4-6]. Accordingly, it is of practical significance to study the mechanical behavior of coral sand under repeated loading.

To date, a number of studies on the mechanical characteristics of silica sand have been conducted [2, 7-14].In addition, data concerning coral materials are abundant [15-19]. Coral sand is characterized by irregular shapes, low unit weights, easily cementing, high porosity, and high permeability[16, 20-23], which are significantly different from the characteristics of general continental and marine sediments [5, 12, 15]. Furthermore, in recent decades, the mechanical properties and evolution of particle breakage of coral sand have been investigated through ring shearing tests [24, 25], conventional triaxial tests [26, 27], one-dimensional compression tests [28-30] and impaction tests [19, 31]. However, only a few investigations have focused on the mechanical properties and particle breakage of coral sand under repeated loading [2, 17, 32-37]. For coral sand in the South China Sea, failure under repeated loading is governed not only by the development of excess pore water pressure but also by the accumulation of axial deformation [17]. He et al. [38], who conducted a series of high-cycle drained triaxial tests on coral sand, found that the accumulated axial strain has a strong correlation with repeated stress paths and critical strength lines, and established empirical formulas for calculating the ultimate strain and stiffness. Wang et al. [39] conducted an in-depth investigation of the effects of the loading mode and effective confining pressure on the strain softening behavior and shear strength angle of coral sand by performing repeated

triaxial loading-unloading tests. Nevertheless, the unique mechanical properties (e.g., particle breakage) of coral sand under repeated loading were not taken into account.

In consideration of the above issues, a series of one-dimensional compression tests are conducted under repeated loading to reveal the compressive characteristics of the coral sand. The volumetric deformation, soil stiffness, and particle breakage of coral sand are carefully measured and discussed. Furthermore, the differences in the compressive properties between silica sand and coral sand are investigated. Finally, it is found that the volumetric deformation and particle breakage of the coral sand can be predicted by using three power functions.

2. Materials and method

The two testing materials used in this study are coral sand taken from an offshore reef in the South China Sea and silica sand commonly used in civil engineering (Fujian standard sand). The curves of the initial grain size distribution are shown in Fig. 1(a), showing that both have the same mean particle diameter (D_{50}=0.6). Scanning electron micrographs of the sand used in this study are presented in Figs. 1(b-c), which show that the silica sand is relatively round and smooth. In contrast, the coral sand is angular and rough. Furthermore, to quantitatively evaluate the particle morphology, the median values of the flatness ratios, elongation ratios, convexity, and angularity indices of silica sand are calculated as 0.36, 0.34, 0.71, and 0.53, respectively, and these values for coral sand are calculated as 0.78, 0.45, 0.45, and 0.28, respectively [40-44]. The physical parameters of these soils are listed in Table 1.

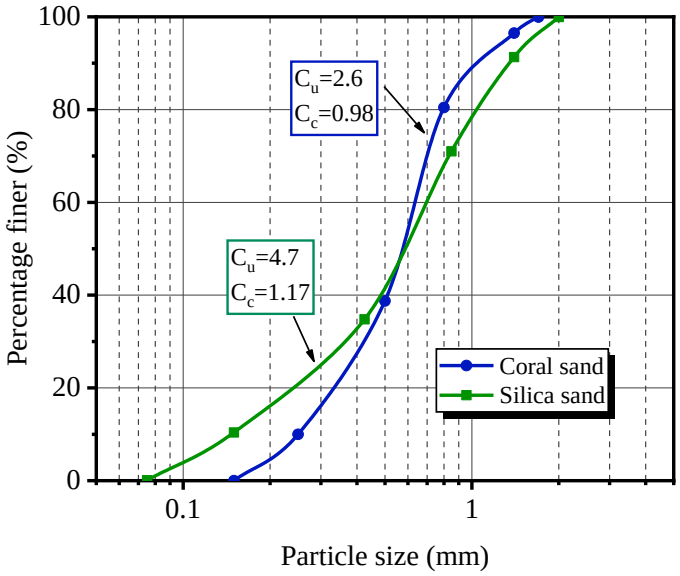

(a)

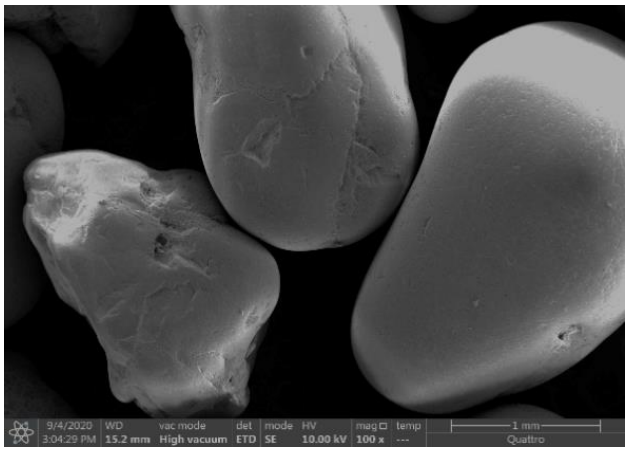

(b)

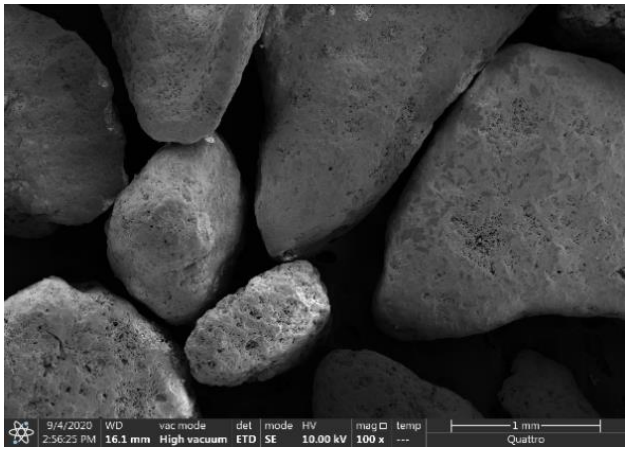

(c)

Figure 1 (a) Initial grain-size distribution; (b) Scanning electron microscopy of the silica sand; (c) Scanning electron microscopy of the coral sand.

Table 1. Sand Parameters

Property	Coral sand	Silica sand
Maximum dry density, γ_{max} : g/cm^3	1.62	1.69
Minimum dry density, γ_{min} : g/cm^3	1.22	1.56
Specific gravity, G_s	2.81	2.63
Maximum void ratio, e_{max}	1.3	0.69
Minimum void ratio, e_{min}	0.72	0.56

Mean particle diameter, D_{50}: mm	0.6	0.6
Uniformity coefficient, C_u	2.6	4.7
Coefficient of curvature, C_c	0.98	1.17
Initial friction angle, φ: °	42	32

Three-repeated compression tests are carried out on 60 sand samples with various initial relative densities and loading amplitudes. The testing apparatus of the one-dimensional compression test is shown in Fig. 2(a), and a linear variable differential transformer (LVDT) is adopted to measure the vertical deformation of the sand sample. The sand sample is a standard cylinder sample with 61.9 mm in diameter and 20 mm in height. Three initial relative densities (25%, 50%, and 75%) and three vertical loading amplitudes (1.6 MPa, 2.4 MPa, and 3.2 MPa) are adopted in this study. The void ratios of coral sand corresponding to the initial relative densities of the design are 1.16, 1.02, and 0.87, which are greater than the void ratios of 0.78, 0.7, and 0.63 in silica sand samples, respectively. The relative density of the design is attained by the quality control method [19, 45]. The sand with the required quality is homogeneously poured into the specimen container in three stages. The calculated qualities for coral sand samples with the three design densities are 78.26 g, 83.68 g, and 90.39 g, and the quantities for silica sand are 88.88 g, 93.06 g, and 97.06 g, respectively. The repeated loading process is illustrated in Fig. 2(b). The loading method is the slow-load maintenance method with the same loading and unloading classifications. Moreover, each sub-loading interval is maintained for 25 min to prevent the creep effect and to ensure the stability of vertical deformation [46, 47]. To ensure the reliability of the testing results, the mean measurements of three sand samples under the same loading conditions are taken as the representative values for analysis and discussion. Coral sand is a granular material that is easy to break [20]. The gradation of coral sand after

loading can be obtained by a soil sieve, and the particle breakage index proposed by Einav [48] is used to quantitatively evaluate the crushability by comparing the gradation curves before and after repeated loading. Because particle breakage is an unrecoverable plastic behavior, and the soil structure of the loaded sand sample will be destroyed during the sieving process, the sieved sand sample cannot be loaded again. Therefore, the same sand samples are subjected to repeated loading with different loading numbers, and then the particle breakage produced in each loading process could be obtained by subtracting the breakage index of the sand sample with a high loading number from that of the sand sample with a low loading number.

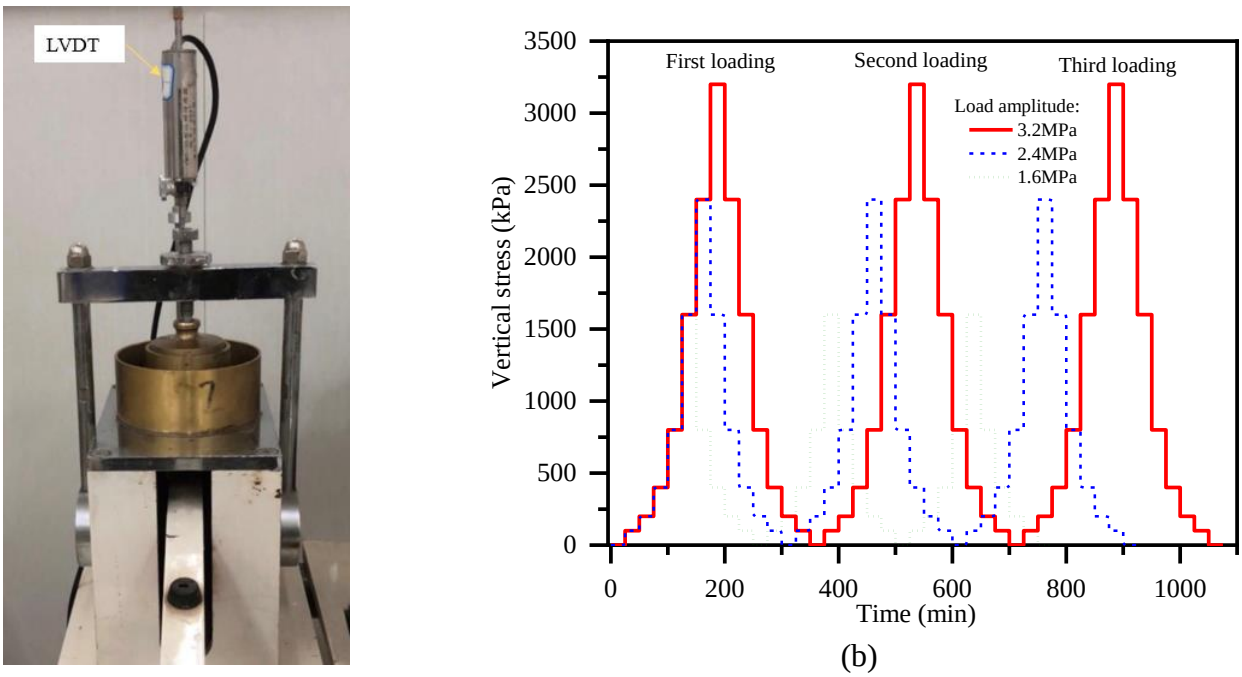

Figure 2 (a) Testing apparatus of the one-dimensional compression test; (b) Repeated loading process.

3. Results and analysis

Figs. 3(a-b) plot the volumetric strain against vertical stress for the two materials. In the legend, the letters C and S are the abbreviations for coral and silica sand respectively, and the middle numerals and the last numerals denote the initial relative density and the vertical stress amplitude, respectively. It is clearly that

the slopes of the curves in the stress range of 0-400 kPa are clearly smaller than those in the stress range of 400-3200 kPa. This can be explained by the fact that the deformation of the sand sample is mainly caused by particle compaction and the reduction in intergranular porosity in the stress range of 0-400 kPa. When the stress level is higher than 400 kPa, it is more difficult to produce further particle compaction because the sample is already compacted in the stress range of 0-400 kPa. Therefore, the deformation at a higher stress stage is mainly caused by particle crushing, resulting in the soil stiffness and the curve slopes being greater than those at a lower stress level. It is evident that the compression behavior of coral sand under repeated loading is significantly different from that of silica sand, and the influence of the initial relative densities and vertical loading amplitude cannot be ignored.

During the tests, the interlocking between particles occurs in coral sand during compression owing to its irregular shape and rough surface. As shown in Fig. 3(c), the coral sand sample becomes a compact sand cake, and the original shape can be maintained after the bottom constraint is removed. In contrast, once the bottom constraint is removed after compression, the silica sand sample collapses (Fig. 3(d)).

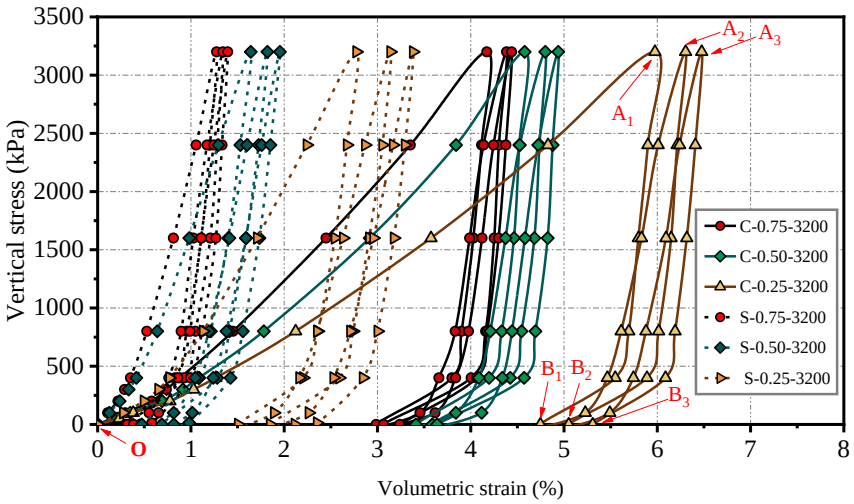

(a)

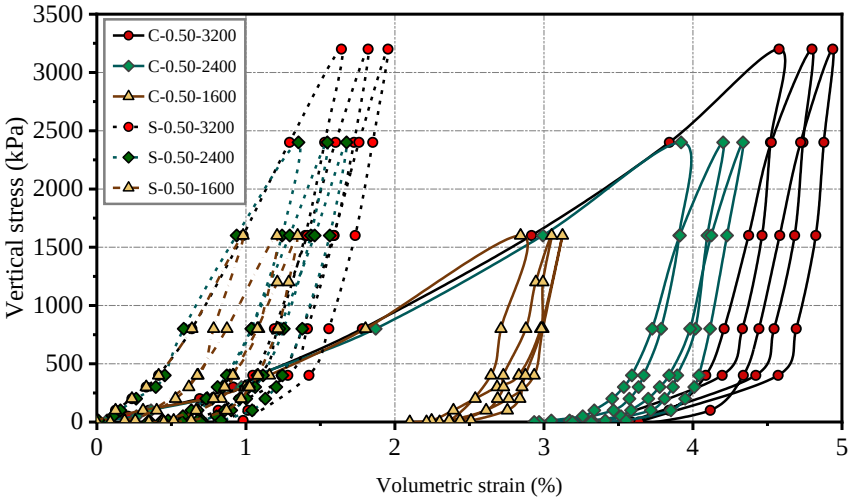

(b)

(c)

(d)

Figure 3 Test results and phenomena: (a) The relationships between σ_v and ε_v for different initial relative densities; (b) The relationships between σ_v and ε_v for different loading amplitudes; (c) Coral sand sample after compressing; (d) Silica sand sample after compressing.

3.1 Volumetric deformation

It is well known that volumetric deformation consists of recoverable elastic deformation and irrecoverable plastic deformation. In the repeated loading process, the accumulated deformation (ε_{o-A_1}, ε_{o-A_2} and ε_{o-A_3} in Fig. 3(a)), deformation in each loading stage (ε_{o-A_1}, $\varepsilon_{B_1-A_2}$ and $\varepsilon_{B_2-A_3}$ in Fig. 3(a)), and increment of accumulated deformation ($\varepsilon_{A_1-A_2}$ and $\varepsilon_{A_2-A_3}$ in Fig. 3(a)) produced in each loading stage are of interest. Fig. 4 shows the volumetric deformation under repeated loading. It should be noted that in the legend of

Figs. 4(a-b), the first letter denotes the type of volumetric strain (T and R represent the total volumetric strain and residual volumetric strain, respectively); the middle letters C and S are the abbreviations for the coral sand and silica sand, respectively; and the last numerals are the number of repeated loading cycles. In Figs. 4(c-d), the middle numerals and the last numerals denote the initial relative density and vertical stress amplitude, respectively.

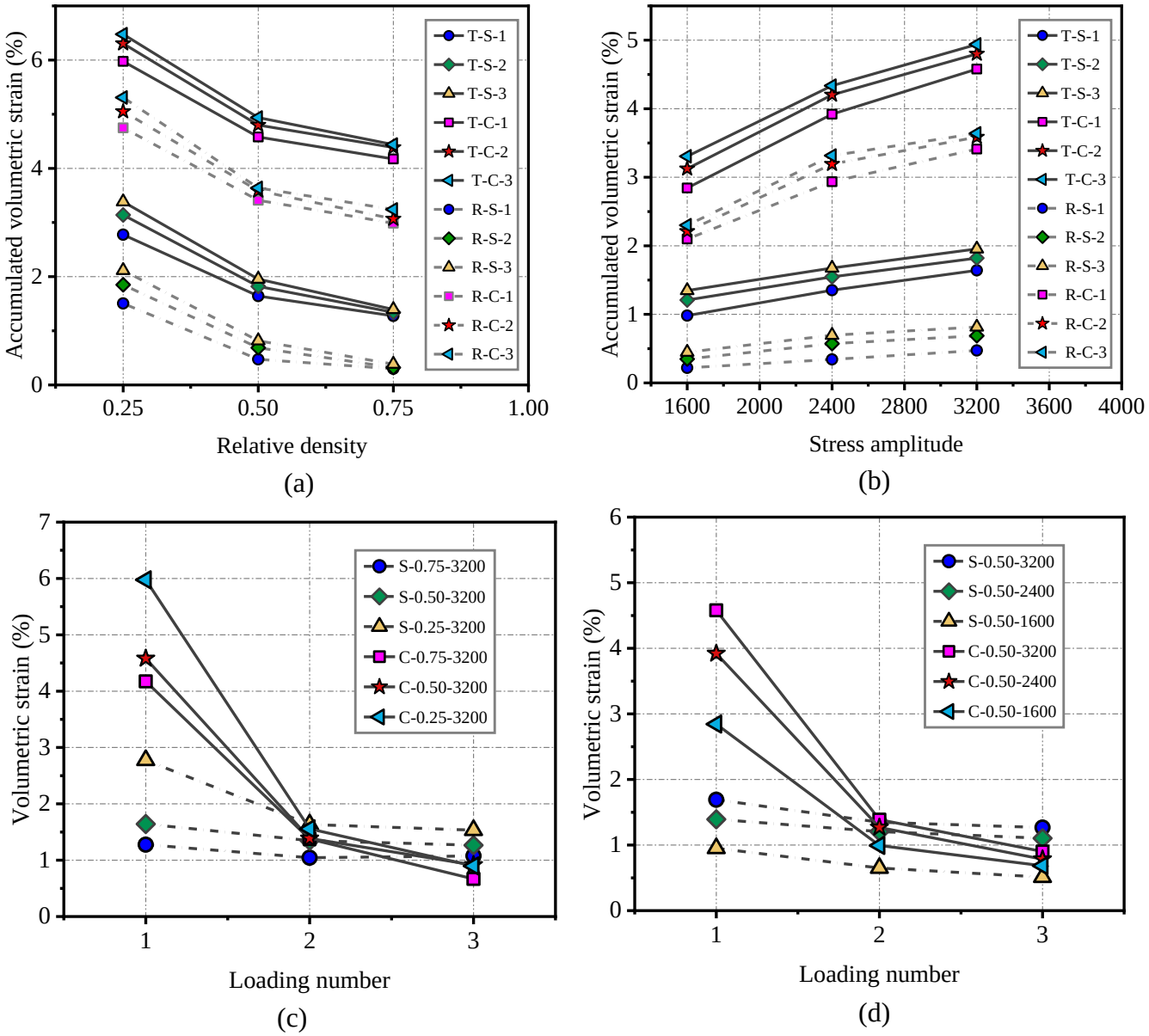

Figure 4 Volumetric deformation: (a) Accumulated volumetric strain versus relative density; (b) Accumulated volumetric strain versus loading amplitude; (c) Volumetric strain in each loading for different relative densities; (d) Volumetric strain in each loading for different loading amplitudes.

It can be clearly seen from Figs. 4(a-b) that the accumulated volumetric strains increase with the number of repeated loading cycles, and most of the deformation occurs in the first loading process. Moreover, the deformation of coral sand is mainly irrecoverable plastic deformation, which accounts for approximately 74% of the total deformation, while the ratio of plastic deformation in silica sand is only 37%. In Figs. 4(c-d), the volumetric strain produced in each loading stage shows a decreasing trend with increasing loading number, indicating that the ability to resist deformation is gradually improved. The volumetric strains of coral sand in the first loading stage are found to be much larger than those of silica sand, and the volumetric strains of coral sand produced in each loading stage gradually decrease by increasing the loading number. Until the loading number is more than three, the deformation of coral sand produced in each loading is even smaller than that of silica sand. This demonstrates that the compressive ability of coral sand can be improved more significantly under repeated loading compared to that of silica sand. From this, we can infer that the settlement of foundations built with coral sand as filler is much larger than that of silica sand foundations, but repeated preloading, as a foundation treatment method, can quickly and effectively improve the bearing capacity of coral sand foundations.

Relative density and stress amplitude are two important factors that affect the compression properties of sand. The volumetric strains increase significantly by increasing the loading amplitude and reducing the relative density (see Figs. 4(c-d)). For instance, when the relative density increases from 0.25 to 0.5 and then to 0.75, the total volumetric strains of coral sand in the first loading stage decrease by 23.4% and 30.16%, respectively, which are smaller than the decrements of silica sand (40.8% and 54.01%). In addition, by increasing the loading amplitude from 1600 kPa to 3200 kPa, the volumetric strain of coral sand in the first loading increase by 61.3% from 2.84% to 4.58%, which is smaller than the increase in silica sand (increase by 77.9%). The influence on sand deformation caused by the relative density and stress amplitude

is more significant in the silica sand sample than that in coral sand sample. Moreover, the volumetric strain in each loading cycle exhibits a decreasing trend with increasing relative density and reducing loading amplitude. For example, when the relative density of coral sand is 0.25, the volumetric strains produced in each loading are 5.97%, 1.56%, and 0.90%, which are larger than those of the sand sample with a relative density of 0.75 (4.17%, 1.38%, and 0.67%). The same trend is observed for the residual strains. It is worth noting that the influence of the relative density and stress amplitude on the coral sand will gradually weakens as the loading number increases; therefore, the volumetric strain produced in each loading cycle tends to the same value under different loading conditions, as shown in Figs. 4(c-d).

3.2 Soil stiffness

It is well known that the void ratio of coral sand is greater than that of silica sand. In the stress range of 0-400 kPa, the deformation of sand sample is mainly caused by particle compaction and the reduction in intergranular porosity, which is dominated by the initial void ratio. Therefore, we only analyze the average soil stiffness with a stress level higher than 400 kPa to prevent the influence of the initial void ratio in this study. Within the stress range of 400-3200 kPa, the average stress increment required to generate per unit volumetric deformation is defined as the compression stiffness, and the average stress decrement required to recover per unit elastic deformation is defined as the unloading stiffness. The evolution of the soil stiffness under repeated loading is presented in Fig. 5.

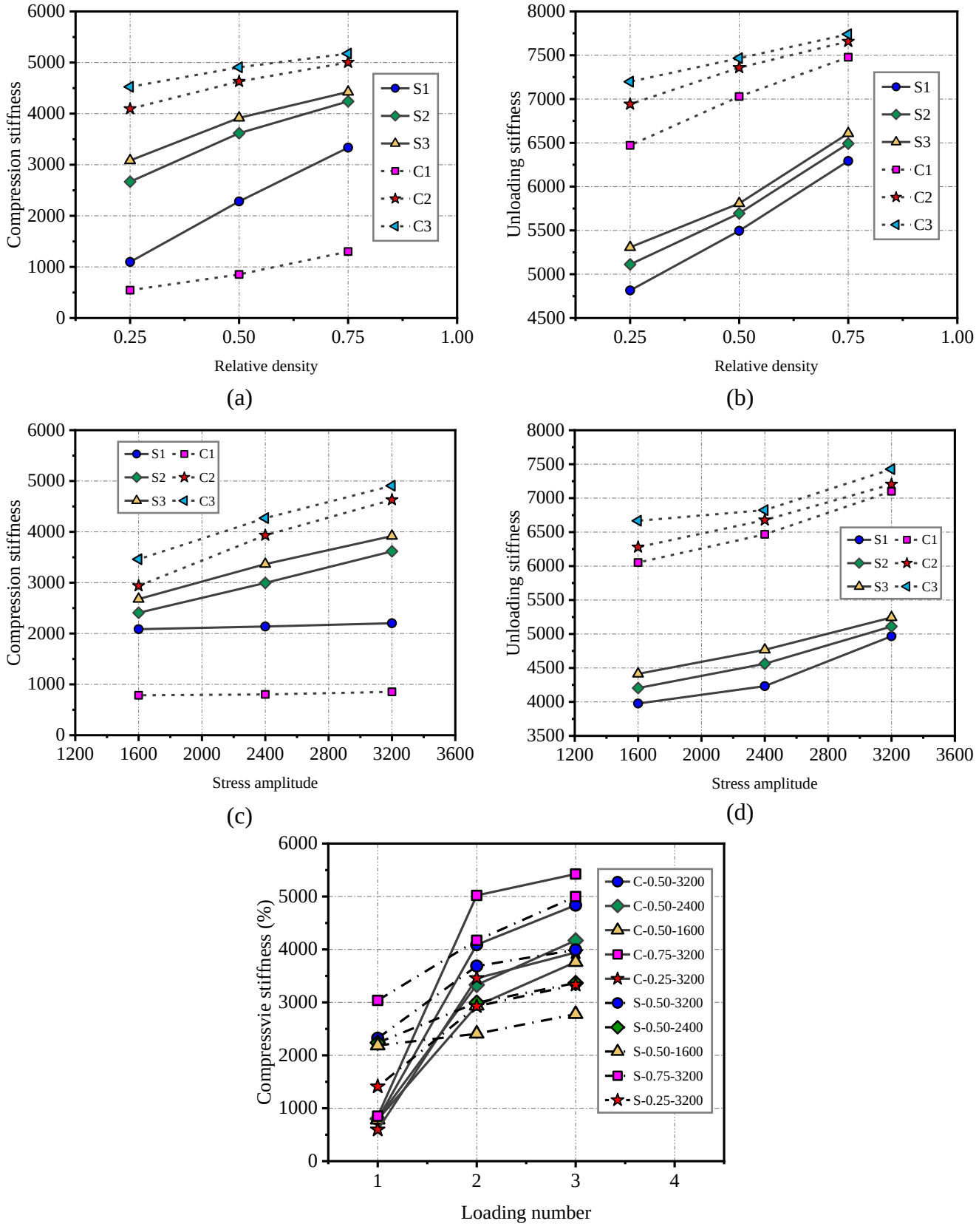

Figure 5 The evolution of soil stiffness under repeated compression: (a) Compressive stiffness versus relative density; (b) Unloading stiffness versus relative density; (c) Compressive stiffness versus loading amplitude; (d) Unloading stiffness versus loading amplitude; (e) Compressive stiffness versus loading number.

Both the compressive and unloading stiffness increase with the loading number, but the growth rate gradually decreases. For example, the compressive stiffness of C-0.5-3200 in the first loading is 794.2 kPa, which gradually increases to 4087.8 kPa and 4834.6 kPa by 4.15 times and 5.08 times by increasing loading number, respectively. The unloading stiffness is greater than the compressive stiffness in coral sand, but the influence of the loading number on the compressive stiffness is more significant than that of the unloading stiffness. The unloading stiffness of C-0.5-3200 is 7100.6 kPa in the first loading stage, and it only increases by 1.5% and 4.6% to 7203.8 kPa and 7426.6 kPa with increasing loading number, respectively. A similar trend as that discussed above can be found for silica sand, but the soil stiffness of coral sand is greater than that of silica sand except for the initial compressive stiffness, implying that the increase in the compressive stiffness under repeated loading is more significant in coral sand than that in silica sand. Therefore, we can conclude that even with low initial compressive stiffness, coral sand is a good filling material because its bearing performance after repeated preloading treatment is better than that of silica sand foundations.

An increase in the initial relative density can significantly improve soil stiffness. The denser the sand sample, the greater the soil stiffness, and the more significant the increase in the soil stiffness as the loading number increases. As shown in Fig. 5(e), by increasing the initial relative density of coral sand from 0.25 to 0.5 and 0.75, the compressive stiffness after three loadings increases from 3942.4 kPa to 4834.6 kPa and 5424.6 kPa, respectively. With the exception of the initial compressive stiffness, which is not affected by the loading amplitude and tends to maintain a constant value, the soil stiffness also increases with increasing loading amplitude. For instance, the compressive stiffness of coral sand increases by 10.9% and 28.6% from 3760 kPa to 4169.4 kPa and 4834.6 kPa when the loading amplitude increases from 1600 kPa to 2400 kPa and 3200 kPa, respectively. Therefore, the initial density and loading amplitude are two

significant factors that can improve the soil stiffness and bearing capacity of coral sand foundations under repeated loading.

3.3 Particle breakage

The particle breakage behavior is a unique property of coral sand that can affect its mechanical properties. In this study, because of the rationality of the concept of the ultimate grain size distribution [49, 50], the breakage index proposed by Einav [48] (see Fig. 6(a)) is adopted to quantify the particle breakage of coral sand by comparing the gradation curves before and after repeated loading. The evolution of the grading for coral sand under repeated loading is shown in Fig. 6(b).

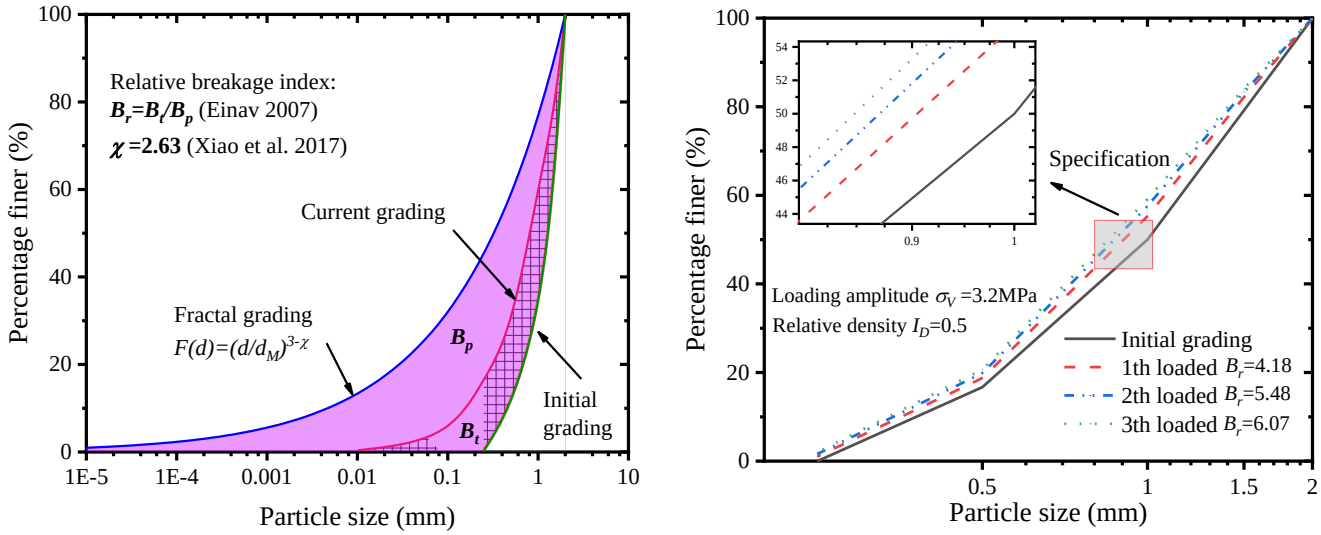

Figure 6 (a) Definition of relative breakage index Br; (b) Evolution of the grading for coral sand under repeated loading.

Figs. 7(a-b) show the evolution of the accumulated particle breakage of coral sand under repeated loading. It is obvious that the accumulated particle breakage increases with decreasing initial density and with increasing loading number and amplitude. For instance, the particle breakage index of C-0.5-3200 is 4.18% after the first loading and unloading stage, which increases to 6.03% after the third loading and unloading

stage is completed. The accumulated particle breakage of C-0.5-3200 after three repeated loadings increases from 6.03% to 6.91% when the relative density decreases to 0.25 and decreases to 3.19% when the loading amplitude decreases to 1600 kPa.

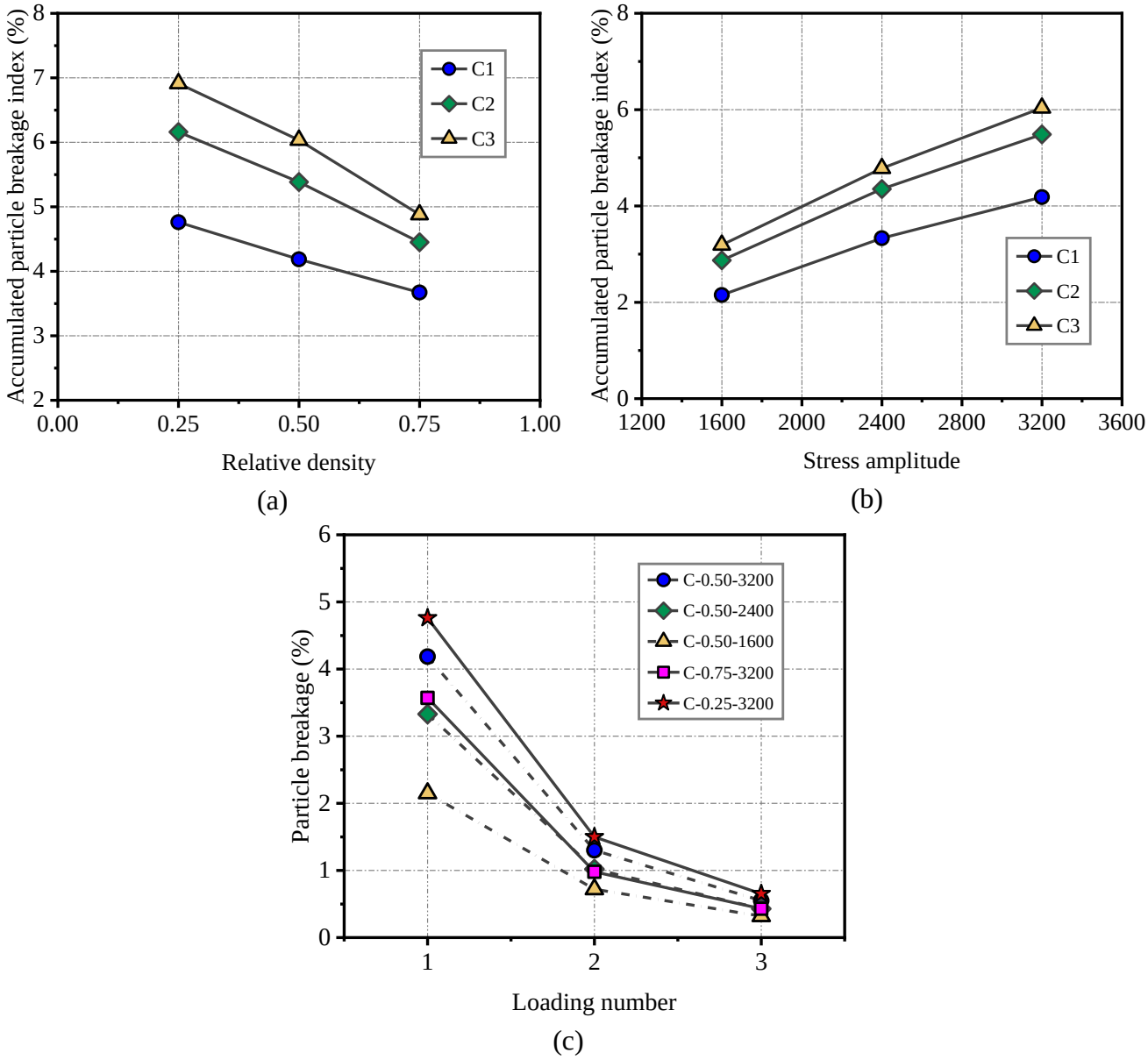

Figure 7 Particle breakage of coral sand: (a) Variations of accumulated particle breakage with initial relative density; (b) Variations of accumulated particle breakage with loading amplitude; (c) Variations of particle breakage with loading number.

Fig. 7(c) shows that the particle breakage produced in each loading stage obviously decreases with increasing loading number, and most particle breakage occurs during the first loading process. C-0.5-3200

is taken as an example, and the particle breakage index in each loading reduces from 4.18% to 1.3% and 0.55% with the increase of loading number, respectively. This indicates that, in the coral sand foundation, the influence of particle breakage under working conditions can be ignored as long as a proper foundation treatment method is adopted prior to working.

Moreover, the particle breakage in each loading stage demonstrates a decreasing trend by increasing the initial relative density. This finding is in agreement with the conclusion in previous studies that the greater the sand density is, the smaller the particle crushing [28, 30]. In addition, increasing the loading amplitude can increase the particle breakage. For example, the particle breakage of C-0.5-1600 in the second loading stage is 0.72%, which increases to 1.02% and 1.3% when the loading amplitude increases to 2400 kPa and 3200 kPa, respectively. However, the loading amplitude and relative density only have a significant effect on particle breakage at the initial loading stage. The influence gradually weakens with increasing loading number, and the breakage tends to be consistent after three loadings. This can be attributed to the fact that the sand sample gradually transitions into a stable compacted state with increasing loading number. After the sufficient preloading treatment, the influence of the initial condition on the particle breakage of coral sand no longer becomes predominant, and particle breakage can be ignored.

4. Discussion

4.1 Volumetric strain

Subgrade settlement is an important problem that must be considered in foundation design. Xiao et al. [26] presented a power function (Eq. (1)) to simulate the relationship between the volumetric deformation, vertical loading stress and relative density of uniform coral sand under compressive loading.

$$\varepsilon_{v}^{0} = (0.97 - 0.59 I_D)(\sigma_V / p_a)^{0.8} / 100 \quad (1)$$

where ε_{v}^{0} is the volumetric strain of uniform coral sand after the first loading stage, I_D initial relative

density, σ_V vertical stress level, and p_a atmospheric pressure. Based on Xiao's function, two parameters are introduced in this study to consider the effects of non-uniform gradation and repeated loading and to quantitatively evaluate the deformation of coral sand under repeated loading:

$$\varepsilon_{vn}' = n^{\chi} \cdot \varepsilon_{v1} = k_g \cdot n^{\chi} \cdot \varepsilon_v^0 = 0.468 \cdot n^{-3.825} \cdot (0.97 - 0.59 I_D)(\sigma_V / p_a)^{0.8} / 100 \quad (2)$$

where ε_v^0 and ε_{v1} are the volumetric strains of uniform and non-uniform coral sand after the first loading stage, respectively, for example, $\varepsilon_{v1} = \varepsilon_{o\text{-}A_1}$ in Fig. 3(a); ε_{vn}' is the increment of the accumulated volumetric strain of non-uniform coral sand produced in the n-th loading process, for example, $\varepsilon_{v3}' = \varepsilon_{A_2\text{-}A_3}$ in Fig. 3(a), k_g is the gradation parameter, n is the number of repeated loads, and χ is the loading parameter.

Fig. 8 shows the relationship between ε_{v1} and ε_v^0, which can be described by a linear fitting curve with a slope of k_g=0.468. This confirms the observation in previous studies that greater volumetric deformations are obtained for uniform coral sand than for non-uniform coral sand [30].

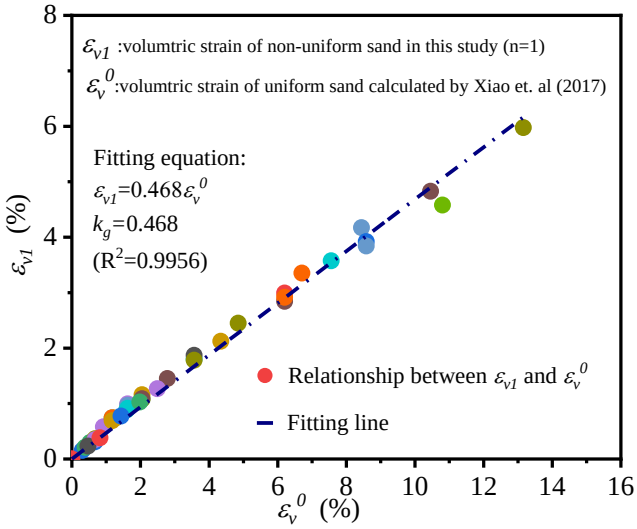

Figure 8 The relationship between ε_{v1} and ε_v^0 for uniform and non-uniform coral sand.

The variation in the strain increment measured in this test with the change in the loading number is shown

in Fig. 9(a), and the loading parameter is equal to -3.825 (R^2=0.9985). As shown in Fig. 9(b), the predictions obtained by using Eq. (2) are in remarkably good agreement with the test data. Therefore, the accumulated volumetric deformation of coral sand under repeated loading can be effectively predicted by using the following fitting equation:

$$\varepsilon_{\mathrm{v}}^{n}=\sum_{n=1}^{n}\varepsilon_{\mathrm{vn}}{}'=\sum_{n=1}^{n}k_g\cdot n^{\chi}\cdot\varepsilon_{\mathrm{v}}^{0}=\sum_{n=1}^{n}0.468\cdot n^{-3.825}\cdot(0.97-0.59I_D)(\sigma_V/p_a)^{0.8}/100 \tag{3}$$

where $\varepsilon_{\mathrm{v}}^{n}$ is the accumulated volumetric deformation of the non-uniform coral sand after the n-th loading stage, for example, $\varepsilon_v^3=\varepsilon_{\mathrm{o\text{-}A_3}}$ in Fig. 3(a).

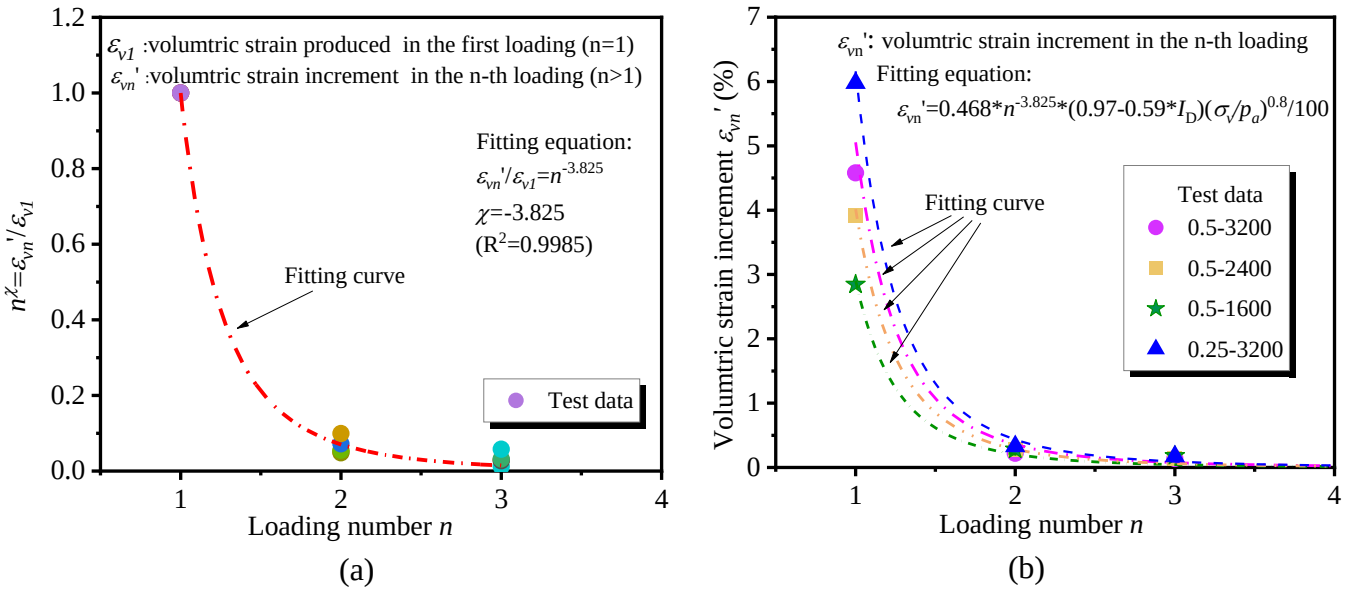

Figure 9 Volumtric deformation of coral sand under repeated loading: (a) The variation of volumetric strain increment with the number of repeated loading cycles ; (b) Verification of Eq. (2).

Fig. 10(a) shows that the volumetric strain produced in each loading stage exhibits an exponentially decreasing trend with increasing number of repeated loading stages, and the loading parameter is equal to -1.645 (R^2=0.9964), which confirms the observation above that the soil stiffness increases with the increase in the loading number. Therefore, the volumetric strain in each loading stage can be obtained by using the following function:

$$\varepsilon_{\mathrm{vn}} = n^{\chi_1} \cdot \varepsilon_{\mathrm{v1}} = k_g \cdot n^{\chi_1} \cdot \varepsilon_v^0 = 0.468 \cdot n^{-1.645} \cdot (0.97 - 0.59 I_D)(\sigma_V / p_a)^{0.8} / 100 \quad (4)$$

where ε_{vn} is the volumetric strain of the non-uniform coral sand produced in the n-th loading process, for example, $\varepsilon_{\mathrm{v3}} = \varepsilon_{\mathrm{B_2\text{-}A_3}}$ in Fig. 3(a).

As shown in Fig. 10(b), the predictions obtained by using Eq. (4) are in remarkably good agreement with the test data, in terms of the relationship between the volumetric strain produced in each loading stage, the loading amplitude, the initial density, and the number of repeated loading stages. Consequently, this function can become a starting point for predicting the settlement of coral sand foundations under repeated wave or traffic loading in the design of practical engineering applications.

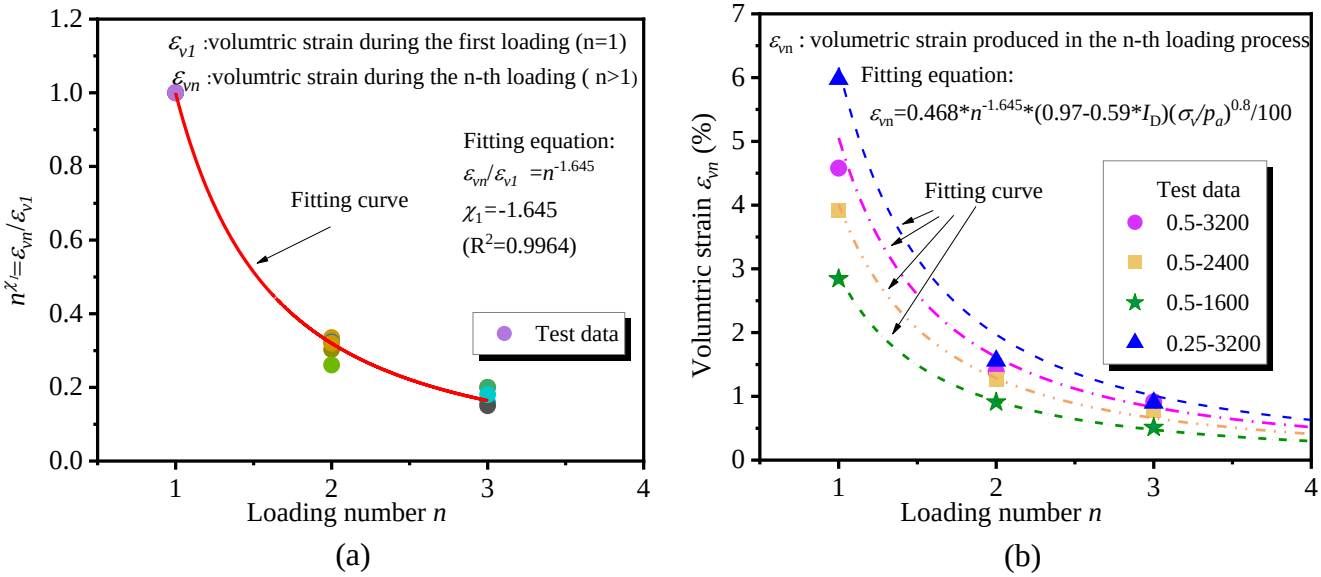

Figure 10 Volumtric deformation of coral sand under repeated loading: (a) The variation of volumetric strain with the number of repeated loading cycles; (b) Verification of Eq. (4).

4.2 Particle breakage

Fig. 11(a) shows the relationship between the relative breakage index B_r and volumetric strain ε_v under repeated loading. It is observed that the test data under various loading conditions are locating in a narrow band, implying that the volumetric strain could intrinsically pertain to particle breaking. The fitting curve for the test data can be described in the form of a power expression:

$$B_r = k_B \cdot \varepsilon_v^{\lambda_B} \tag{5}$$

where k_B and λ_B are material constants with values of 0.58 and 1.25, respectively.

Eq. (4) is substituted into Eq. (5), and the relationship between the particle breakage of coral sand, loading amplitude, initial relative density and loading number under repeated loading is derived as follows:

$$B_{rn} = 0.58 \cdot (\varepsilon_{vn})^{1.25} = 0.58 \cdot \left[0.468 \cdot n^{-1.645} \cdot (0.97 - 0.59 I_D)(\sigma_V / p_a)^{0.8} / 100 \right]^{1.25} \tag{6}$$

where B_{rn} is the particle breakage produced in the n-th loading process.

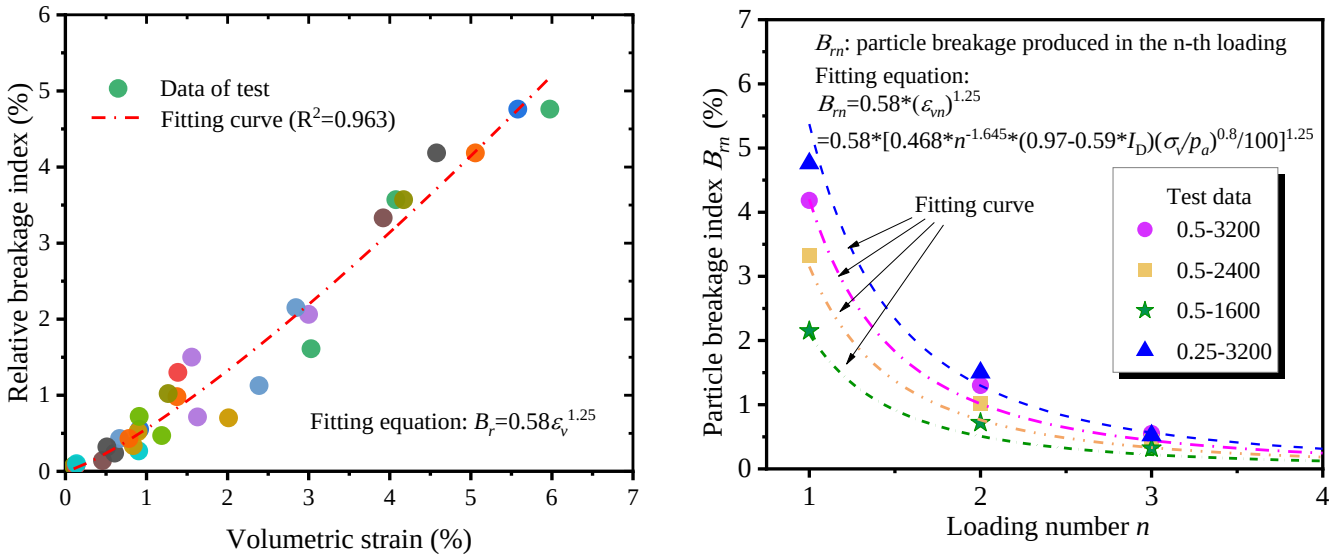

Figure 11 Particle breakage of coral sand under repeated loading: (a) Relationship between relative breakage index and volumetric strain; (b) Verification of Eq. (6).

Fig. 11(b) shows the verification of Eq. (6), illustrating that the prediction calculated by using Eq. (6) agrees well with the test data. Therefore, this function could become a new method for evaluating the influence of particle breakage in practical engineering application. Eq. (6) shows that the particle breakage index is less than 0.5% after five loading stages, and the influence of particle breakage can be ignored.

5. Conclusions

This paper presents an experimental study on the compressive characteristics and particle breakage of coral

sand to provide a valuable reference for the engineering design of coral sand foundations under repeated loading. The main findings are summarized as follows:

(1) The deformation of coral sand mainly occurs during the first loading process, and the ratio of plastic deformation is approximately 74%, which is larger than the value of 37% observed in silica sand. In addition, the influence of the initial condition (relative density and stress amplitude) gradually decrease as the loading number increases.

(2) The soil stiffness of the coral sand is lower than that of silica sand during the initial loading process. However, the opposite trend is observed for the subsequent loading. In addition, the soil stiffness increases significantly with increasing initial relative density, loading amplitude and number, and the improvement is more significant in coral sand.

(3) Under repeated loading, the particle breakage of the coral sand increases significantly with a reduction in the initial relative density and an increase in the loading amplitude, but the influence gradually weakens with increasing loading number. Particle breakage mainly occurs in the first loading stage, and the breakage index in each loading stage exhibits a decreasing trend with increasing loading number.

(4) A unique relationship between the volumetric strain and the particle breakage of coral sand is observed. Furthermore, the accumulated volumetric strain, volumetric strain, and particle breakage of coral sand in each loading stage can be described by power-type functions, which are dependent on the loading amplitude, initial relative density, and loading number.

Acknowledgments

This work is supported by the National Natural Science Foundation of China (Grant Nos. 51878103 and 51778092), and Innovation Group Science Fundation of the Natural Science Fundation of Chongqing, China (Grant No. cstc2020jcyj-cxttX0003).

References

[1] Houlsby G. (2016) Interactions in offshore foundation design. Géotechnique 66 1-35.

[2] Pincus H.J., Lo Presti D.C.F., Pallara O., Lancellotta R., Armandi M., Maniscalco R. (1993) Monotonic and Cyclic Loading Behavior of Two Sands at Small Strains. Geotech. Test. J. 16(4).

[3] Ding X., Zhang Y., Wu Q., Chen Z., Wang C. (2021) Shaking table tests on the seismic responses of underground structures in coral sand. Tunnelling and Underground Space Technology 109.

[4] Luan L., Ding X., Zheng C., Kouretzis G., Wu Q. (2020) Dynamic response of pile groups subjected to horizontal loads. Can. Geotech. J. 57(4) 469-481.

[5] Luan L., Zheng C., Kouretzis G., Ding X. (2020) Dynamic analysis of pile groups subjected to horizontal loads considering coupled pile-to-pile interaction. Comput. Geotech. 117(Jan.) 103276.1-103276.8.

[6] Ding X., Qu L., Yang J., Wang C. (2020) Experimental study on the pile group-soil vibration induced by railway traffic under the inclined bedrock condition. Acta Geotech. (1–5).

[7] Xiao Y., Yuan Z., Lv Y., Wang L., Liu H. (2018) Fractal crushing of carbonate and quartz sands along the specimen height under impact loading. Construction and Building Materials 182 188-199.

[8] Wu M., Wang J. (2019) Registration of point cloud data for matching crushed sand particles. Powder Technol. 347 227-242.

[9] Huang J., Xu S., Hu S. (2013) Effects of grain size and gradation on the dynamic responses of quartz sands. International Journal of Impact Engineering 59 1-10.

[10] Ovalle C., Dano C., Hicher P.-Y., Cisternas M. (2015) Experimental framework for evaluating the mechanical behavior of dry and wet crushable granular materials based on the particle breakage ratio. Can. Geotech. J. 52(5) 587-598.

[11] Danha G., Legodi D., Hlabangana N., Bhondayi C., Hildebrandt D. (2016) A fundamental investigation on the breakage of a bed of silica sand particles: An attainable region approach. Powder Technol. 301 1208-1212.

[12] Lv Y., Li F., Liu Y., Fan P., Wang M. (2017) Comparative study of coral sand and silica sand in creep under general stress states. Can. Geotech. J. 54(11) 1601-1611.

[13] Xiao Y., Meng M., Daouadji A., Chen Q., Wu Z., Jiang X. (2020) Effects of particle size on crushing and deformation behaviors of rockfill materials. Geosci. Front. 11(2) 375-388.

[14] Muir Wood D., Maeda K. (2008) Changing grading of soil: Effect on critical states. Acta Geotech. 3 3-14.

[15] Lv Y., Liu J., Xiong Z. (2019) One-dimensional dynamic compressive behavior of dry calcareous sand at high strain rates. J. Rock Mech. Geotech. Eng. 11(1) 192-201.

[16] Ma L., Li Z., Wang M., Wei H., Fan P. (2019) Effects of size and loading rate on the mechanical properties of single coral particles. Powder Technol. 342 961-971.

[17] Wang Y., Qiu Y., Ma L., Li Z. (2019) Experimental study on the cyclic response of Nanhai Sea calcareous sand in China. Arabian Journal of Geosciences 12(22).

[18] Lv Y., Wang Y., Zuo D. (2019) Effects of particle size on dynamic constitutive relation and energy absorption of calcareous sand. Powder Technol. 356 21-30.

[19] Peng Y., Ding X., Xiao Y., Deng X., Deng W. (2020) Detailed amount of particle breakage in multi-sized coral sands under impact loading. European Journal of Environmental and Civil Engineering 10.1080/19648189.2020.1762750 1-10.

[20] Konrad J., Salami Y. (2018) Particle breakage in granular materials — a conceptual framework. Can.

Geotech. J. 55(5) 710-719.
[21] Zhu C., Liu H., Zhou B. (2016) Micro-structures and the basic engineering properties of beach calcarenites in South China Sea. Ocean Engineering 114 224-235.
[22] Xiao Y., Desai C.S., Daouadji A., Stuedlein A.W., Liu H., Abuel-Naga H. (2020) Grain crushing in geoscience materials–Key issues on crushing response, measurement and modeling: Review and preface. Geosci. Front. 11(2) 363-374.
[23] Peng Y., Liu H., Li C., Ding X., Deng X., Wang C. (2021) The detailed particle breakage around the pile in coral sand. Acta Geotech. 10.1007/s11440-020-01089-2.
[24] Coop M.R., Sorensen K.K., Bodas Freitas T., Georgoutsos G. (2004) Particle breakage during shearing of a carbonate sand. Géotechnique 54(3) 157-163.
[25] Miao G., Airey D. (2013) Breakage and ultimate states for a carbonate sand. Géotechnique 63(14) 1221-1229.
[26] He S.-H., Zhang Q.-F., Ding Z., Xia T.-D., Gan X.-L. (2020) Experimental and Estimation Studies of Resilient Modulus of Marine Coral Sand under Cyclic Loading. Journal of Marine Science and Engineering 8(4).
[27] Shahnazari H., Rezvani R. (2013) Effective parameters for the particle breakage of calcareous sands: An experimental study. Engineering Geology 159 98-105.
[28] Xiao Y., Liu H., Chen Q., Ma Q., Xiang Y., Zheng Y. (2017) Particle breakage and deformation of carbonate sands with wide range of densities during compression loading process. Acta Geotech. 12(5) 1177-1184.
[29] Peng Y., Ding X., Xiao Y., Deng X., Deng W. (2019) Detailed amount of particle breakage in non-uniformly graded sands under one-dimensional compression. Can. Geotech. J. 57(8) 1239-1246.
[30] Wang C., Ding X., Xiao Y., Peng Y., Liu H. (2021) Effects of relative densities on particle breaking behaviour of non-uniform grading coral sand. Powder Technol. https://doi.org/10.1016/j.powtec.2021.01.015.
[31] Xiao Y., Liu H., Xiao P., Xiang J. (2016) Fractal crushing of carbonate sands under impact loading. Geotech. Lett. 6(3) 199-204.
[32] Airey D., Fahey M. (1991) Cyclic response of calcareous soil from the North-West Shelf of Australia. Geotechnique 41 101-121.
[33] Kaggwa W.S., Booker J.R., Carter J.P. (1991) Residual Strains in Calcareous Sand due to Irregular Cyclic Loading. Journal of Geotechnical Engineering 117(2) 201-218.
[34] Hyodo M., Aramaki N., Itoh M., Hyde A. (1996) Cyclic strength and deformation of crushable carbonate sand. Soil Dynamics and Earthquake Engineering 15 331-336.
[35] Lackenby J., Indraratna B., McDowell G., Christie D. (2007) Effect of confining pressure on ballast degradation and deformation under cyclic triaxial loading. Géotechnique 57(6) 527-536.
[36] Salem M., Elmamlouk H., Agaiby S. (2013) Static and cyclic behavior of North Coast calcareous sand in Egypt. Soil Dynamics and Earthquake Engineering 55 83-91.
[37] Ding Z., He S.-H., Sun Y., Xia T.-D., Zhang Q.-F. (2021) Comparative study on cyclic behavior of marine calcareous sand and terrigenous siliceous sand for transportation infrastructure applications. Construction and Building Materials 283.
[38] He S., Ding Z., Xia T.-D., Zhou W.-H., Gan X., Chen Y.-Z., Xia F. (2020) Long-term behaviour and degradation of calcareous sand under cyclic loading. Engineering Geology 276 105756.
[39] Wang X., Cui J., Zhu C.-Q., Wu Y., Wang X. (2021) Experimental study of the mechanical behavior of calcareous sand under repeated loading-unloading. Bulletin of Engineering Geology and the

Environment 80.
[40] Blott S.J., Pye K. (2007) Particle shape: a review and new methods of characterization and classification. Sedimentology 0(0) 070921092734002-???
[41] Bagheri G.H., Bonadonna C., Manzella I., Vonlanthen P. (2015) On the characterization of size and shape of irregular particles. Powder Technol. 270 141-153.
[42] Kong D., Fonseca J. (2018) Quantification of the morphology of shelly carbonate sands using 3D images. Géotechnique 68(3) 249-261.
[43] Xiao Y., Long L., Evans T.M., Zhou H., Stuedlein A.W. (2019) Effect of Particle Shape on Stress-Dilatancy Responses of Medium-Dense Sands. Journal of Geotechnical and Geoenvironmental Engineering 145(2) 04018105.
[44] Wang C., Liu H., Ding X., Wang C., Ou Q. (2021) Study on the horizontal bearing characteristics of pile foundation in coral sand. Can. Geotech. J. http://dx.doi.org/10.1139/cgj-2020-0623.
[45] Peng Y., Ding X., Xiao Y., Deng X., Deng W. (2019) Detailed amount of particle breakage in non-uniformly graded sands under one-dimensional compression. Can. Geotech. J. 10.1139/cgj-2019-0283.
[46] Shipton B., Coop M.R. (2012) On the compression behaviour of reconstituted soils. Soils and Foundations 52(4) 668-681.
[47] Zhou M., Song E. (2016) A random virtual crack DEM model for creep behavior of rockfill based on the subcritical crack propagation theory. Acta Geotech. 11(4) 827-847.
[48] Einav I. (2007) Breakage mechanics—Part I: Theory. Journal of the Mechanics and Physics of Solids 55(6) 1274-1297.
[49] Huang Q., Zhou W., Ma G., Ng T.-T., Xu K. (2020) Experimental and numerical investigation of Weibullian behavior of grain crushing strength. Geosci. Front. 11(2) 401-411.
[50] Mao W., Aoyama S., Towhata I. (2020) A study on particle breakage behavior during pile penetration process using acoustic emission source location. Geosci. Front. 11(2) 413-427.